

Topsy-turvy locomotion: biomechanical specializations of the elbow in suspended quadrupeds reflect inverted gravitational constraints

Shin-ichi Fujiwara,^{1,2} Hideki Endo¹ and John R. Hutchinson²

¹The University Museum, The University of Tokyo, Tokyo, Japan

²Structure and Motion Laboratory, The Royal Veterinary College, London, UK

Abstract

Some tetrapods hang upside down from tree branches when moving horizontally. The ability to walk in quadrupedal suspension has been acquired independently in at least 14 mammalian lineages. During the stance (supportive) phase of quadrupedal suspension, the elbow joint flexor muscles (not the extensors as in upright vertebrates moving overground) are expected to contract to maintain the flexed limb posture. Therefore muscular control in inverted, suspended quadrupeds may require changes of muscle control, and even morphologies, to conditions opposite to those in upright animals. However, the relationships between musculoskeletal morphologies and elbow joint postures during the stance phase in suspended quadrupeds have not been investigated. Our analysis comparing postures and skeletal morphologies in *Choloepus* (Pilosa), *Pteropus* (Chiroptera), *Nycticebus* (Primates) and *Cynocephalus* (Dermoptera) revealed that the elbow joints of these animals were kept at flexed angles of 70–100 ° during the stance phase of quadrupedal suspension. At these joint angles the moment arms of the elbow joint flexors were roughly maximized, optimizing that component of antigravity support. Our additional measurements from various mammalian species show that suspended quadrupeds have relatively small extensor/flexor ratios in both muscle masses and maximum moment arms. Thus, in contrast to the pattern in normal terrestrial quadrupeds, suspended quadrupeds emphasize flexor over extensor muscles for body support. This condition has evolved independently multiple times, attendant with a loss or reduction of the ability to move in normal upright postures.

Key words: elbow; flexor muscle; fruit bat; lorises; quadrupedal suspension; sloth.

Introduction

Some tetrapods can move horizontally below the substrate in an inverted (dorsal-side down) position using all four limbs. This is called quadrupedal suspension (Napier, 1967). The ability to use quadrupedal suspension has evolved at least 14 times in at least eight clades of extant mammals: Diprotodontia (*Tarsipes*), Pilosa (*Bradypus*, *Choloepus*, *Cyclopes* and *Tamandua*), Primates (*Pongo*, *Ateles*, *Potto* and *Nycticebus*), Rodentia (*Glirulus*, *Graphiurus*, *Petaurista* and *Pteromys*), Scandentia (*Tupaia*), Chiroptera (*Pteropus* and *Rousettus*), Dermoptera (*Cynocephalus*) and Carnivora (*Nasua*, *Potos* and *Bassariscus*) (Grassé, 1955; Mendel, 1981, 1985; Russell, 1986; Cant, 1987; Jouffroy & Petter, 1990;

McClearn, 1992; Trapp, 1972; Sargis, 2001; Youlatos, 2002; Airapetyants & Fokin, 2003; Thorpe & Crompton, 2006; Lim, 2007). Some squamate reptiles such as *Gekko* (Gekkonidae) and *Chamaeleo* (Chamaeleonidae) employ quadrupedal suspension as well (Autumn et al. 2002; Losos et al. 1993). Among extinct animals, the locomotion of some extinct primates, such as palaeopropithecids, often is reconstructed in quadrupedal suspension (e.g. Godfrey & Jungers, 2003).

Animals must generate mediolateral torques with their limbs to balance above a thin branch (Lammers & Gauntner, 2008), whereas they can be stable without this torque when in suspension (Napier, 1967). Notably, many suspended quadrupeds maintain their elbow in a flexed pose during the stance (foot in contact with substrate; supportive) phase or in static postures (Grassé, 1955; Mendel, 1981, 1985; Jouffroy & Petter, 1990; Lim, 2007; Thorpe & Crompton, 2006; Nyakatura et al. 2010). This condition differs from brachiation in gibbons, spider monkeys and orangutans, in which the elbows are fully extended in suspension (Jungers & Stern, 1980, 1981; Thorpe & Crompton, 2006), although the forelimb bones still experience considerable tensile strains

Correspondence

Shin-ichi Fujiwara, The University Museum, The University of Tokyo, 7-3-1 Hongo, Bunkyo-ku, Tokyo 113-0033, Japan. E: sinitchy@um.u-tokyo.ac.jp or sfujiwara@rvc.ac.uk

Accepted for publication 18 March 2011
Article published online 8 April 2011

(Swartz et al. 1989) as likely is the case for suspended quadrupeds. Neither the elbow extensor nor the flexor muscles are active during the stance phase of brachiation (Jungers & Stern, 1980, 1981), whereas the elbow flexors contract during the stance phase of quadrupedal suspension (Jouffroy & Stern, 1990) against an extensor torque incurred by the downward gravitational force (Fig. 1; also Ishida et al. 1990).

'Normal' (dorsal-side up) upright quadrupedal postures are opposite to quadrupedal suspension in both the orientation of the trunk and the activity patterns of elbow joint muscles. In these postures, elbow joint extensor muscles contract to counter moments imposed by the ground reaction force during the stance phase (e.g. Cohen & Gans, 1975; Jenkins & Weijs, 1979; Tuttle et al. 1983; Jouffroy & Stern, 1990; Gregersen et al. 1998; Wickler et al. 2005), and the elbows are kept at an angle where the moment arms of the extensors are nearly maximized (Fujiwara, 2009). This matching of limb postures to moment arm magnitude, irrespective of other critical determinants of support such as muscle force, force-length or force-velocity properties, or moment arms of external forces, concurs with the hypothesis that animals often use nearly optimal muscle moment arms as a control target for effective support (e.g. Lieber, 1997; Hutchinson et al. 2005; Johnson et al. 2008). But does this hypothesis apply to unusually specialized animals, such as suspended quadrupeds?

The unusual mechanics and presumed differences of muscular control in quadrupedal suspension pose other interesting questions about musculoskeletal adaptation, such as

how well matched the morphology of elbow flexors is to the demands of quadrupedal suspension. This question could be answered by quantifying the relationship between the elbow angle and the musculoskeletal morphology such as moment arms (leverages of elbow muscles). It is striking that the biomechanics of this unusual locomotor strategy, in which the direction of gravitational pull is inverted relative to the dorsoventral body axis, has hardly been investigated. In contrast, theories about the relation between posture and muscular support have been formulated for many non-inverted animals (e.g. Alexander, 1984; Biewener, 1989, 1990, 2005; Kram & Taylor, 1990; Dickinson et al. 2002; Reilly et al. 2007). Quadrupedal suspension provides a marvellous opportunity to examine how phylogenetic history (i.e. ancestry from animals that did not use quadrupedal suspension) and functional constraints (i.e. conflicting demands for resisting gravitational forces in normal vs. inverted poses) have influenced locomotor form and function. Has evolution resulted in suspended quadrupeds with near-optimal matches between morphology (i.e. elbow flexor muscle moment arms) and behaviour (i.e. elbow postures)? Or have functional constraints or phylogenetic baggage resulted in compromises in which suboptimal moment arms are used, perhaps because muscle force output or external moments constrain the usage of such postures?

To answer these questions we conducted a broad comparative study of elbow joint musculoskeletal form and function during quadrupedal suspension in four taxa that have convergently evolved this locomotor style, and employed comparisons with animals that do not move in

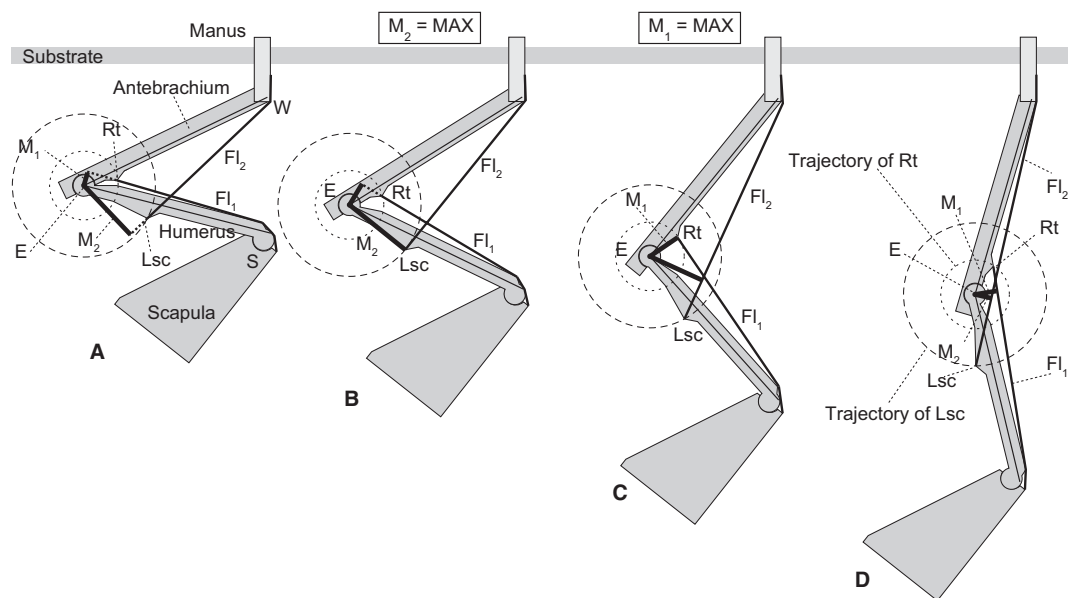


Fig. 1 Model of forelimb mechanics during quadrupedal suspension in various elbow joint angles from (A) flexed to (D) extended. The elbow is subject to an extensor torque induced by body weight and resisted by counteracting muscle forces times moment arms (M_n). M_2 and M_1 are maximized at the specific elbow joint angle shown in (B) and (C), where the lines E-Lsc and E-Rt are perpendicular to Fl_2 and Fl_1 , respectively. E, centre of elbow joint rotation; Fl_1 and Fl_2 , flexor muscle groups along the brachium and antebrachium, respectively; M_1 and M_2 , moment arms of Fl_1 and Fl_2 , respectively; Lsc, lateral supracondylar crest; Rt, radial tuberosity; S and W, shoulder and wrist joints, respectively.

inverted, quadrupedally suspended poses. We attached importance especially to limb bone geometry, with an eye to applying our findings to reconstructions of limb postures in extinct animals in the future.

Hypothetical flexor moment arms of the elbow joint

Generally, there are two groups of elbow joint flexor muscles: one runs nearly parallel to the humeral shaft (Fl_1), such as *M. biceps brachii* and *M. brachialis*, and the other nearly parallel to the antebrachium (Fl_2), such as *M. extensor carpi radialis* and *M. brachioradialis* (Fig. 1). The former group inserts into the radial tuberosity (Rt) and the latter group originates from the lateral supracondylar crest (Lsc; Fig. 1). The flexor torque (τ) about the elbow joint created by muscle(s) is:

$$\tau_n = M_n \times F_n$$

where F_n is the force vector of Fl_n and M_n is a moment arm of the Fl_n (perpendicular line from the centre of elbow joint rotation E to the muscle Fl_n ; Fig. 1A–D). A greater elbow flexor torque is created by the muscle (τ_n) when the moment arm M_n or the scalar quantity of the muscle force F_n gets larger. The value of M_n is measurable from dissection, whereas the muscle force (F_n) is more difficult to determine but can be approximated by muscle mass (see Methods). M_1 is maximized at the angle where the Fl_1 is perpendicular to the line connecting E and Rt (Fig. 1C), whereas M_2 is maximized at the angle where Fl_2 is perpendicular to the line connecting E and Lsc (Fig. 1B).

Based on the above mechanical considerations, we hypothesize that the elbow joints during the stance phases of quadrupedal suspension are maintained close to the angle(s) where the moment arms of flexor muscles (M_1 , M_2) are maximized. Our second hypothesis is that, in contrast to the general condition in normal, non-suspended taxa, the elbow flexor muscles in suspended quadrupeds are more developed than the extensors, having both greater moment arms and masses. To test our two hypotheses, we compared the elbow joint angles *in vivo* during quadrupedal suspension (measured from videos) with those angles at which the flexor moment arms are maximized (estimated from skeletal geometry). We also compared the maximum possible moment arms and actual muscle masses of elbow joint flexors and extensors across a wide diversity of mammals (100 specimens, 67 genera).

Materials and methods

Comparison between observed and estimated elbow joint angles

The elbow joint angles observed *in vivo* for quadrupedal suspension and the angles estimated to maximize muscle moment

arms (from skeletons) were compared to each other in four taxa of different mammalian clades: the two-toed sloth (*Choloepus*; Pilosa), fruit bat (*Pteropus*, Chiroptera), colugo (*Cynocephalus*, Dermoptera) and slow loris (*Nycticebus*, Primates). The measurements of both observed and estimated elbow joint angles were taken from one to two species for each genus. Here we assume that interspecific variation within a genus (whether caused by inherited or environmental factors, including captivity) is relatively small, which our qualitative observations from external and skeletal anatomy as well as dissections support. Although we lack sufficient sample size to test this assumption statistically, it should not influence our general, qualitative results and conclusions.

The changes of elbow joint angle during the stance phases of quadrupedal suspension for 16 step cycles (strides) in total were collected for *Choloepus hoffmanni* ($n = 6$), *Pteropus dasymallus* ($n = 6$) and *Nycticebus coucang* ($n = 4$) at the Ueno Zoo (Tokyo, Japan). The angles were measured from lateral view video clips (30 Hz video; FVM300, Canon, Japan). Orientations of forelimb skeletal elements *in vivo* are generally difficult to observe through the surrounding soft tissues. However, our dissections and radiographs of *Choloepus* and *Nycticebus* demonstrated that the cranial (flexor) margin of the upper arm and the line connecting the olecranon and the ulnar edge of the wrist joint are nearly parallel to the shaft of the humerus and antebrachium, respectively, and thus these boundaries can be used as a proxy for the orientations of forelimb elements (Fig. 2). In *Pteropus* and *Cynocephalus*, the shoulder, the elbow and the wrist positions are quite recognizable through the membrane that covers the forelimb, so the elbow joint angle was measured between the lines from the shoulder to the elbow and wrist joint centres.

Animals were moving at steady, normal walking speeds. Speeds were not measured for this study due to lack of consistent scale objects in the field of view to calibrate distances, but qualitatively were very consistent and speeds did not vary obviously among trials.

An additional problem our analysis encountered was that the actual elbow joint angles could not be very accurately determined from lateral view video footage when the humerus was abducted (Fig. S1). Humeral abduction and antebrachial supination occur during the first half of the stance phase. These out-of-sagittal plane motions obscure the flexion/extension angle of the elbow. They are followed by humeral adduction and pronation during the latter half in *Choloepus* and *Nycticebus* (S.-I. Fujiwara, personal observation), which facilitated more reliable quantification of joint angles. Therefore in our analysis we separated the abducted portion of the stance phase from the adducted portion, and emphasize the latter here.

The static elbow joint angles during rest were also measured from lateral view photographs of *C. hoffmanni* ($n = 5$), *P. dasymallus* ($n = 6$), *Nycticebus* [*N. coucang* ($n = 2$), *N. pygmaeus* ($n = 3$)], and *Cynocephalus variegatus* ($n = 4$). We used photographs taken at Ueno Zoo as well as photographs from the literature (Lim, 2007).

The range of elbow joint motion permitted by the musculo-skeletal system was measured from fresh carcasses that we used for this study's dissections: two *Choloepus*, three *Pteropus*, two *Cynocephalus*, and two *Nycticebus* (Table 1). Carcasses that had been deeply frozen were not used for these measurements, nor were specimens that had been fixed or otherwise dehydrated. The original flexibility of the elbow joints was assumed to be

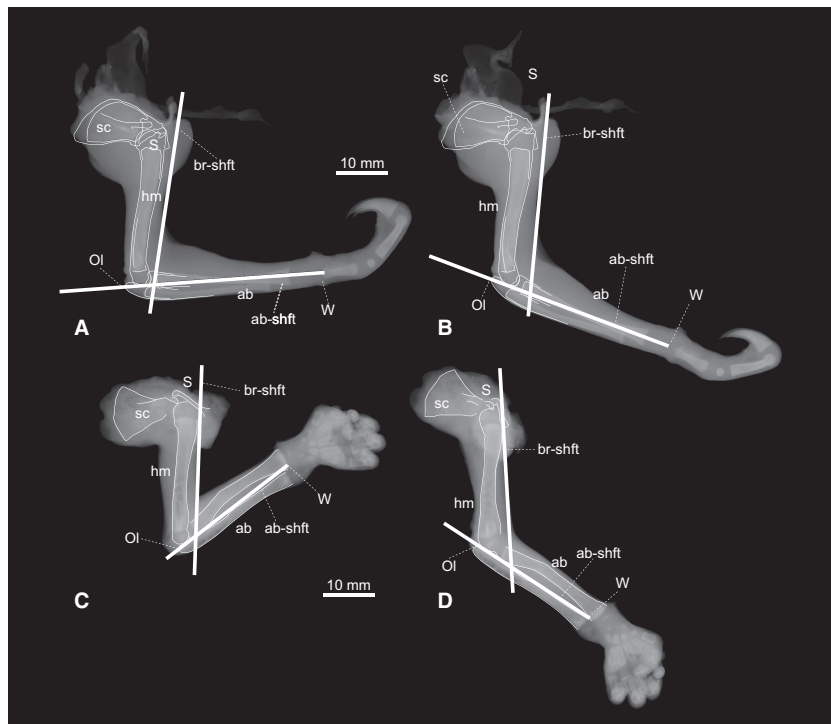


Fig. 2 Radiographs of (A,B) *Choloepus* (UMUT unnumbered) and (C,D) *Nycticebus* (NSM M 35960) forelimbs in (A,C) flexed and (B,D) extended elbow joint angles. The cranial margin of the humerus is assumed to be nearly parallel to the shaft of the humerus (br-shft), and the line connecting the olecranon (Ol) and the wrist joint (W) is assumed to be nearly parallel to the shaft of the antebrachium (ab-shft). ab, antebrachium; hm, humerus; sc, scapula; S and W, shoulder and wrist joints, respectively.

Table 1 Elbow joint angle estimated from skeletons. Elbow joint angles where the moment arms of Fl_1 and Fl_2 (elbow flexors along the brachium and antebrachium, respectively) are maximized, and the range of elbow joint motion (ROM) measured from fresh carcasses is indicated. The mean value (ave.) of each measurement is also indicated for each genus, followed by number of measurements in parentheses.

Genus	Specimen	Fl_1	Fl_2	ROM
<i>Choloepus</i>		ave. 70 ° (n = 5)	ave. 72.2 ° (n = 5)	
<i>C. hoffmanni</i>	NSM M 10137	72 °	71 °	–
	UMUT unnumbered (juvenile)*	72 °	71 °	53–133 °
	UMUT unnumbered*	70 °	74 °	50–120 °
<i>C. didactylus</i>	NSM PO 134	66 °	72 °	–
	IC	70 °	73 °	–
<i>Pteropus</i>		ave. 69.75 ° (n = 4)	ave. 67.75 ° (n = 4)	
<i>P. dasymallus</i>	NSM PO 127	60 °	69 °	–
<i>P. pselaphon</i>	NSM M 34798	76 °	71 °	–
	NSM M 35961*	69 °	65 °	29–118 °
<i>P. sp.</i>	UMUT unnumbered*	74 °	66 °	11–145 °
	UMUT unnumbered*	–	–	14–140 °
<i>Nycticebus</i>		ave. 85.25 ° (n = 4)	ave. 72.25 ° (n = 4)	
<i>N. coucang</i>	NSM M 335	81 °	71 °	–
	NSM M 35960 (juvenile)*	87 °	76 °	59–131 °
	NSM M 36100	87 °	73 °	–
	KPM 3674*	86 °	69 °	59–139 °
<i>Cynocephalus</i>		ave. 68 ° (n = 3)	ave. 66.67 ° (n = 3)	
<i>C. variegatus</i>	ZRC 4.8183*	–	–	28–104 °
	ZRC 4.9464 (juvenile)*	–	–	35–137 °
	ZRC 4.8187	67 °	66 °	–
	ZRC 4.8119	68 °	65 °	–
	ZRC 4.8112	69 °	69 °	–

Institution abbreviations: IC, personal collection of N. Inuzuka, Graduate School of Medicine, The University of Tokyo, Tokyo, Japan; KPM, Kanagawa Prefectural Museum, Odawara, Japan; NSM, National Science Museum, Tokyo, Japan; UMUT, The University Museum, the University of Tokyo, Japan; ZRC, Zoological Collection, Raffles Museum of Biodiversity Research, Singapore.

*Fresh specimens used.

roughly maintained in these specimens. The purpose of this measurement was not to determine precisely the actual range of motion *in vivo*, but to determine where the optimal elbow joint angle estimated from the geometries of bones (below) lay within the range of possible elbow joint motion.

In the next step, we estimated the elbow joint angle where the flexor moment arms are maximized from 18 forelimb skeletons for our study genera (Table 1). The humerus and the antebrachium were photographed in the plane of elbow extension/flexion. The centres of elbow joint rotation (E) was determined from the curvature of the articular surfaces of the trochlea (humerus) and the arc formed by the trochlear notch (ulna) and sagittal crest (radius) of the antebrachium (Figs 1 and 3). To simplify our model, the radius and the ulna were held in semi-supinated positions in *Choloepus* and *Nycticebus*, in accordance with the limb posture during the second half of stance phase (when the humerus is adducted). In *Pteropus* and *Cynocephalus*, the antebrachium has no pronation/supination mobility and is fixed into a semi-supinated position. The Supporting Information contains images that document these non-parasagittal locomotor postures for three of our study genera (*Choloepus*, *Pteropus* and *Nycticebus*: Fig. S1); *Cynocephalus* was only photographed in static poses (see Fig. 4E).

We estimated the optimal elbow joint angle for the moment arms of *M. biceps brachii* (Fl₁; Fig. 1C) and *M. extensor carpi radialis* (Fl₂; Fig. 1B) from the skeletal geometry. The path of Fl₁ was assumed to be the line connecting the surface of the cranial side of the intertubercular groove of the humerus and the radial tuberosity (Rt; Fig. 3A,B). The path of Fl₂ was assumed to be the line connecting the midpoint of the lateral supracondylar crest (Lsc) and the distalmost portion of the radius (Fig. 4A,B). Measurements of moment arms based on the bone geometry are useful when the joint has a single degree of freedom constrained by its pulley action, and the lines of the muscle actions are nearly straight from the origin and the insertion (An et al. 1984). In the elbow joints of mammals, the trochlear notch moves along the arc of the closely fitting trochlea: therefore, the joint axis is not expected to deviate much from point E (Fig. 1). We also confirmed by dissection that, at least in all four study genera, both the distal portion of *M. biceps brachii* (Fl₁) and the proximal portion of *M. extensor carpi radialis* (Fl₂) do not wrap around the elbow joint even when the elbows are fully extended (to their limits of ~ 150°). We validated our assumption that the paths of the flexor muscles approximate straight lines using radiographs (SOFTEX CMB-80; Softex Co., Ltd, National Museum of Nature and Science, Tokyo, Japan) or dissections of fresh carcasses for some specimens (Figs 2 and 4).

Measurements were made using calipers (0–200 mm; Mitutoyo Mfg. Co., Ltd.) and a Martin-type anthropometer (200–1950 mm; Takei Scientific Instruments Co., Ltd.). In the final step of our analysis we compared the observed and the estimated elbow joint angles to test our first hypothesis.

Ratios of flexor/extensor muscle moment arm and muscle mass

For the second part of our analysis we categorized our study specimens into six qualitative groups of forelimb-based locomotor abilities based on the presence or absence of terrestrial quadrupedal abilities [upright (sagittal)/non-upright (crawling or sprawling)] and arboreal abilities [non-scansorial/scansorial (climbing)/quadrupedal suspension]. These categories were:

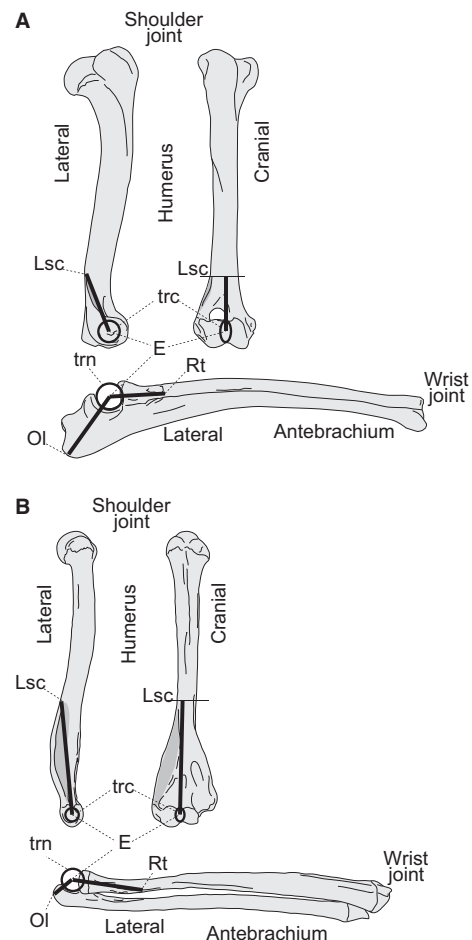


Fig. 3 Measurements of distances E-Ol, E-Rt and E-Lsc used to calculate the maximum possible moment arms of elbow joint extensors and flexors, respectively, along the brachium and antebrachium. (A) Non-scansorial upright quadruped example (*Canis*; Type A). (B) Non-upright suspended quadruped example (*Choloepus*; Type F). See Materials and methods and Fig. 5 for the categories of locomotor ability. E, centre of elbow joint rotation; Lsc, lateral supracondylar crest; Ol, olecranon; Rt, radial tuberosity; trc, trochlea; trn, trochlear notch.

Type A, upright animals with no scansorial abilities; Type B, upright animals with scansorial abilities but with no quadrupedal suspension abilities; Type C, upright animals with quadrupedal suspension abilities; Type D, non-upright animals with no scansorial abilities; Type E, non-upright animals with scansorial abilities but with no quadrupedal suspension abilities; and Type F, non-upright animals with quadrupedal suspension abilities (Fig. 5). We did not distinguish habitual bipeds (e.g. *Macropus*), amphibious (e.g. *Enhydra*), flying (e.g. *Pteropus*), gliding (e.g. *Cynocephalus* and *Petaurista*) or fossorial animals (e.g. *Mogera* and *Dasyus*) from the other mammals, simply emphasizing quadrupedal abilities (Fig. 5). An animal was categorized as a scansorial or suspended quadruped if these behaviours were reported in the literature, but the levels of those abilities were not taken into account because such fine categorization was deemed too arbitrary (Fig. 5; Table 2).

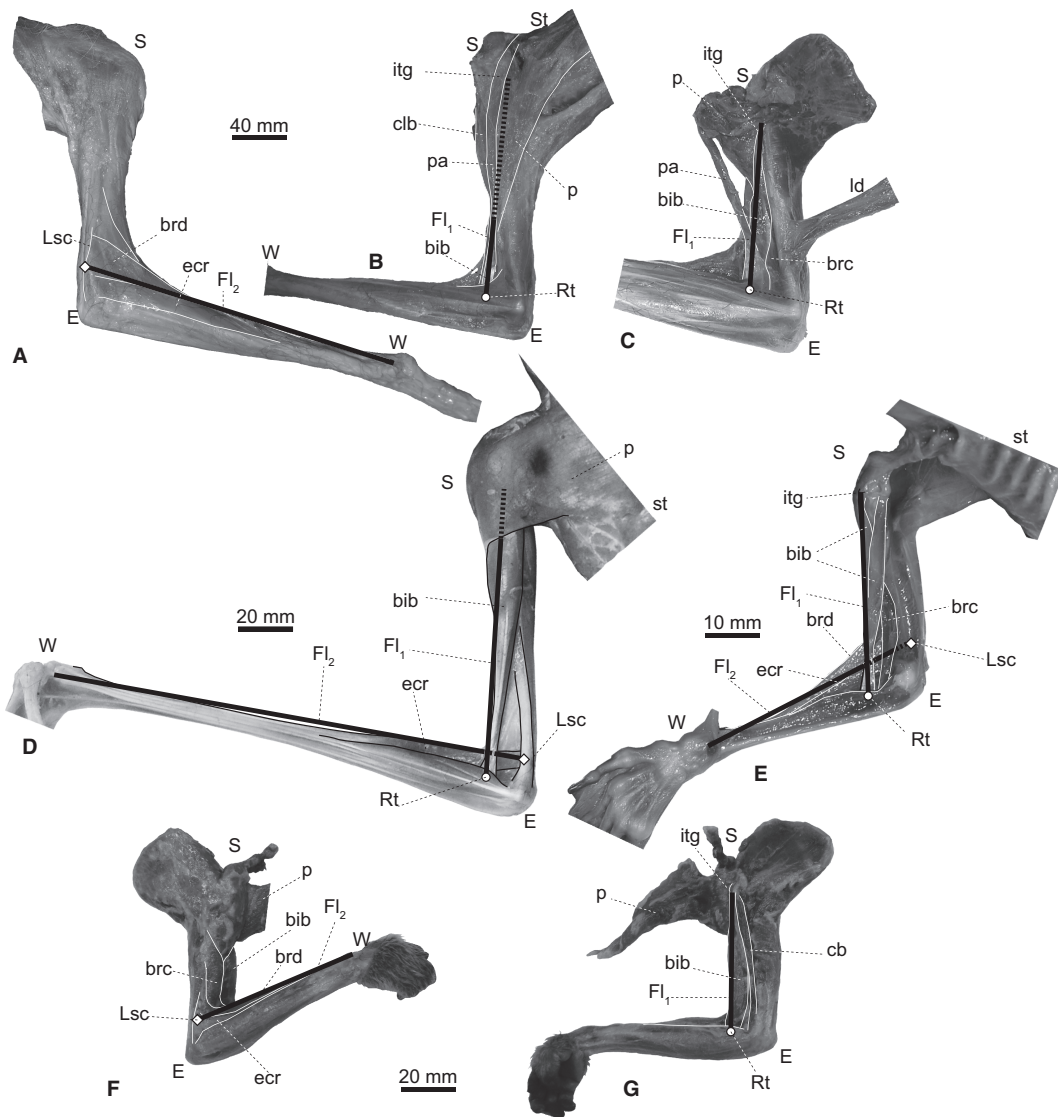


Fig. 4 Elbow joint flexors of (A–C) *Choloepus* (UMUT unnumbered), (D) *Pteropus* (UMUT unnumbered), (E) *Cynocephalus* (ZRC 4.9464) and (F, G) *Nycticebus* (KPM 3684), in lateral (A, F) and medial views (B–E, G). Pectoral muscles are reflected or removed in C, E and G. A flexor muscle along the brachium (FI_1) is represented as a line connecting the inter-tubercular groove (itg) and the radial shaft (Rt). A flexor muscle along the antebrachium (FI_2) is represented as a line connecting the mid-portion of the lateral supracondylar crest (Lsc) and the wrist joint (W). bib, *M. biceps brachii*; brd, *M. brachioradialis*; cb, *M. coracobrachialis*; clb, *M. cleidobrachialis*; ecr, *M. extensor carpi radialis*; ld, *M. latissimus dorsi*; p, *M. pectoralis*; pa, part of *M. pectoralis* which inserts onto the antebrachium; st, sternum; E, S, and W, elbow, shoulder, and wrist joints, respectively. Note that our FI_1 and FI_2 groups best represent the paths of *M. biceps brachii* and *M. extensor carpi radialis*, respectively, but nonetheless are reasonable approximations of the paths, and thus moment arms, of the two major groups of elbow flexor muscles.

The maximum possible moment arms of elbow joint extensor and flexor muscles were measured in dried skeletons and carcasses of 100 mammal specimens representing 67 genera, 40 families and 17 orders (Table 2). We used specimens from KPM (Kanagawa Prefectural Museum, Odawara, Japan), IC (personal collections of N. Inuzuka, Graduate School of Medicine, The University of Tokyo, Japan), NSM (National Science Museum, Tokyo, Japan), UMUT (The University Museum, The University of Tokyo, Japan), UMZC (University Museum of Zoology, Cambridge, UK), and ZRC (Zoological Reference Collection, Raffles Museum of Biodiversity Research, Singapore).

The distance between the centre of elbow joint rotation (E) and the most distant (i.e. caudal) point from E on the olecranon (Ol) was assumed to be a reasonable approximation of the maximum moment arm of the extensors, such as *M. triceps brachii* and *M. dorsiepitrochlealis* (Fig. 3A, B). Similarly, the distances between E and the distalmost point of the Rt or the proximal edge of Lsc were respectively used to estimate the maximum moment arm of FI_1 (*M. biceps brachii*, *M. brachialis*, *M. brachioradialis* and *M. pectoantebrachialis*) and FI_2 (*M. extensor carpi radialis* and *M. brachioradialis*: Fig. 3A, B). Because there were no landmarks on the antebrachium and humerus for determining

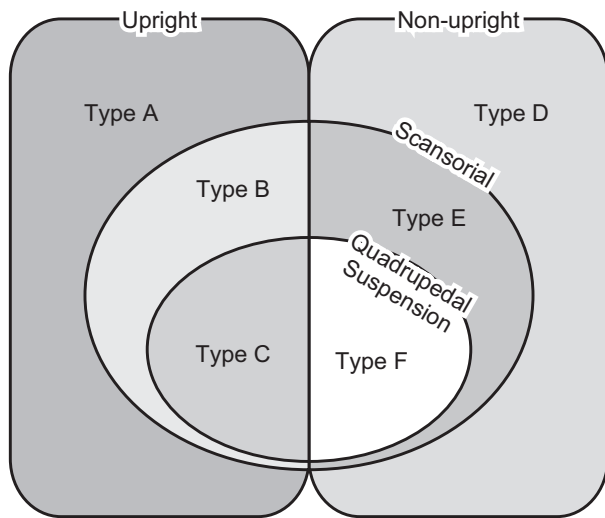


Fig. 5 Locomotor abilities of mammals categorized into six types (see Materials and methods).

the centre of elbow joint rotation (E), we first calculated the radii of the trochlear notch and the trochlea from measurements of their diameters (as above). Next, the distances between E and the most distant point from E on the olecranon (Ol) and the distal-most point of the radial tuberosity (Rt) were calculated by adding the measurement of the minimum length from the margin of the trochlear notch to Ol and Rt, and the radius of the trochlear notch, respectively (Fig. 3A,B). Likewise, the distance between E and the proximal edge of the lateral supracondylar crest (Lsc) was calculated by subtracting the radius of the trochlea from the distance between the distal-most portion of the trochlea and Lsc (Fig. 3A,B). The length 'E-Ol' divided by the length 'E-Rt or E-Lsc, whichever is larger' is defined here as the index of elbow extensor/flexor moment arm ratio.

The masses of the elbow joint extensor and flexor muscles were also measured from fresh carcasses in 37 specimens representing 26 genera (Fig. 6). We used specimens from KPM, NSM, UMUT, ZRC (above), and personal collections of J. R. Hutchinson. These mass measurements were made using an electronic balance (0.001 g of accuracy: Shimadzu Co., Ltd.). The flexor/extensor function of each muscle was determined from dissections by pulling the muscle along its line of action because the functions of homologous muscles are not always the same among taxa [e.g. *M. triceps brachii caput mediale* does not extend the elbow in *Tamandua* (Taylor, 1978)], and also because unusual muscles function as elbow extensors/flexors in some taxa [e.g. *M. pectoantibrachialis*, a pectoral muscle which inserts onto the antibrachium as an elbow flexor in *Choloepus* (Fig. 4B,C; Lucae, 1884)].

Limitations of the analyses

Our methods have several technical limitations yet we contend these should not greatly influence our results. Because the videos were taken only from lateral views, we could not measure the elbow angles throughout the stance phase (Fig. 7) or three-dimensionally (but see Fig. S1). However, our estimates of the elbow joint angle during the latter half of the stance phase in

Choloepus (Fig. 6A) match the measurements by Nyakatura et al. (2010) based on three-dimensional cineradiographs. Specifically, the elbow joint angle is around 60° in mid-stance, and increases to around 110° toward the end of the stance phase (Nyakatura et al. 2010).

We have only sampled four main genera as representatives from four clades that include highly specialized suspended quadrupeds, of at least eight extant clades that use these behaviours. We predict that future studies of clades/genera we have not yet sampled would bolster our results and allow more robust phylogenetic hypotheses to be tested (e.g. the evolutionary sequences that have produced/enabled quadrupedal suspension). However, access to these rare, often endangered species for measurement and dissection will remain an obstacle. Nonetheless, our study is the first broadly comparative analysis of suspended quadrupeds — all previous studies have focused on one species or genus in isolation. Furthermore as noted above, our sample sizes were too small to characterize fully individual variation within species (see Kikuchi, 2010 for an approach that could be conducted with larger samples of our study taxa).

We used a geometric method instead of the tendon travel method (An et al. 1984; Spoor & Van Leeuwen, 1992) or other approaches (e.g. MRI, cineradiography) to quantify the moment arms of muscles, although the latter may provide more accurate data. However, moment arm analyses have previously been conducted using the tendon travel method for the elbow joints in taxa which have similar musculoskeletal geometries to our study taxa. These similarities include that the origins and insertions of the elbow flexor muscles are located near the shaft of the humerus and the antibrachium, respectively. These studies show that the elbow flexor muscle moment arms are maximized at flexed angles of around 90° (*Homo*, *Pan*, *Symphalangus* and *Macaca*: Murray et al. 1995; Thorpe et al. 1999; Graham & Scott, 2003; Michilsens et al. 2010) as in our results (see below). This trend, however, is not observed when the moment arm-joint angle relationships are approximated by straight lines and quadratic equations (e.g. studies of hares and greyhounds by Williams et al. 2007, 2008) but we suspect that this discrepancy may be an artefact of the methods of the latter studies, particularly the quadratic equations, which reduce accuracy for estimating moment arms at some joint angles (Channon et al. 2010). Overall, these published data validate our simple geometric model.

Furthermore, our model focuses on the largest and presumably most important elbow flexors, grouped as Fl₁ (especially *M. biceps brachii*) and Fl₂ (especially *M. extensor carpi radialis*), for our study taxa. Our qualitative observations support our assumption that this focus is justified, because other elbow flexors in groups Fl₁ (e.g. *M. brachialis*, *M. brachiocephalicus*) and Fl₂ (e.g. *M. brachioradialis*) follow roughly parallel lines of action that should give them similar moment arms and moment arm-angle trajectories, and in most cases have nearly identical origins and/or insertions (Fig. 4).

Our dataset of muscle masses alone is insufficient to quantify muscle force outputs fully because it is not the muscle mass but the physiological cross-section area (PCSA) of the muscle that indicates its force-producing capability. However, maximal force output should still correlate strongly with muscle mass. This is because PCSA is proportional to the product of the muscle mass and the cosine of the pennation angle, and is inversely proportional to the product of the density of muscle and the fibre

Table 2 Lists of maximum possible moment arms (in millimetres) of elbow joint flexor muscles along the brachium (Fl₁) and antebrachium (Fl₂), and of the elbow joint extensors (Ex), the extensor/flexor moment arm ratio (MAR), and types of locomotor abilities (LA) in the mammals studied. The Reference column indicates where information on locomotor abilities (LA column) was checked.

Taxonomy			Moment arms (mm)			MAR		
Order/family	Taxa	Specimen	Fl ₁	Fl ₂	Ex	Ex/Fl	LA	References
Monotremata								
Tachyglossidae	<i>Tachyglossus aculeatus</i>	NSM M 28691	11.3	25.4	24.2	0.953	D	Nowak (1999)
Diprotodontia								
Phalangeridae	<i>Trichosurus vulpeculis</i>	NSM M 34964	18.9	14.7	14.4	0.761	B	Weisbecker & Warton (2006)
Phascolarctidae	<i>Phascolarctos cinereus</i>	NSM M 821	35.2	30.2	23.3	0.662	B	Weisbecker & Warton (2006)
Macropodidae	<i>Macropus giganteus</i>	NSM M 35838	56.9	42.4	37.3	0.655	A	Weisbecker & Warton (2006)
	<i>M. giganteus</i>	UMUT unnumbered*	48.6	49.6	38.4	0.774	A	Weisbecker & Warton (2006)
	<i>M. giganteus</i>	UMUT 0140	29.2	21.9	20.8	0.714	A	Weisbecker & Warton (2006)
	<i>M. agilis</i>	UMUT 0047	40.3	27.6	26.1	0.648	A	Weisbecker & Warton (2006)
Afrosoricida								
Tenrecidae	<i>Tenrec ecaudatus</i>	UMZC E.5431.H	11.9	12.4	12.3	0.988	A	Salton & Sargis (2009)
	<i>Setifer setosus</i>	UMZC E.5450.B	7.4	6.9	6.2	0.844	A	Salton & Sargis (2009)
	<i>Hemicentetes nigriceps</i>	UMZC E.5445.B	5.7	6.9	7.5	1.088	A	Salton & Sargis (2009)
Chrysochloridae	<i>Amblysomus hottentotus</i>	UMZC 2010.15.A	3.7	2.3	7.5	2.011	D	Nowak (1999)
Tubulidentata								
Orycteropodidae	<i>Orycteropus afer</i>	NSM M 34334	69.3	27.6	56.3	0.813	A	Nowak (1999)
	<i>O. afer</i>	UMZC E.1326	54.3	33.0	59.4	1.094	A	Nowak (1999)
Hyracoidea								
Procaviidae	<i>Procavia capensis</i>	NSM M 34896	11.2	15.1	16.3	1.079	B	Nowak (1999)
	<i>P. sp.</i>	UMZC E.4980.K	11.4	17.2	15.1	0.878	B	Nowak (1999)
	<i>Dendrohyrax arboreus</i>	UMZC H.5281	7.7	13.0	12.1	0.931	B	Nowak (1999)
Proboscidea								
Elephantidae	<i>Elephas maximus</i>	NSM M 33109	314.0	109.5	262.8	0.837	A	Nowak (1999)
	<i>E. maximus</i>	UMUT 0701	221.7	207.3	168.1	0.758	A	Nowak (1999)
	<i>E. maximus</i>	UMZC H.4611	249.8	293.4	208.4	0.710	A	Nowak (1999)
Cingulata								
Dasypodidae	<i>Dasypus novemcinctus</i>	IC	20.1	8.6	27.7	1.379	A	Nowak (1999)
	<i>Chaetopractus villosus</i>	UMZC E.1062	27.5	11.1	19.2	0.698	A	Nowak (1999)
	<i>Tolypeutes muriei</i>	UMZC E. 1182	11.2	8.5	18.8	1.674	A	Nowak (1999)
	<i>Chlamyphorus truncatus</i>	UMZC E.1201	8.9	2.8	10.5	1.186	A	Nowak (1999)
Pilosa								
Bradyrodidae	<i>Bradypus tridactylus</i>	UMZC E.21	44.9	31.8	11.0	0.245	F	Mendel (1985)
	<i>B. tridactylus</i>	UMZC E.23	45.8	32.9	11.2	0.245	F	Mendel (1985)
Megalonychidae	<i>Choloepus hoffmanni</i>	NSM M 10137	66.5	31.3	15.9	0.239	F	Mendel (1981)
	<i>C. hoffmanni</i>	UMUT unnumbered*	23.6	12.5	7.9	0.249	F	Mendel (1981)
	<i>C. hoffmanni</i>	UMUT unnumbered*	65.2	36.7	16.3	0.335	F	Mendel (1981)
	<i>C. didactylus</i>	NSM PO 134	45.7	55.8	15.5	0.278	F	Mendel (1981)
	<i>C. didactylus</i>	IC	60.7	30.9	14.9	0.245	F	Mendel (1981)
Cyclopedidae	<i>Cyclopes didactylus</i>	UMZC E.621	15.1	9.0	7.7	0.510	C	Nowak (1999)
Myrmecophagidae	<i>Myrmecophaga tridactylus</i>	NSM M 34333	79.7	31.7	52.3	0.657	B	Young et al. (2003)
	<i>Tamandua tetradactyla</i>	NSM M unnumbered*	57.8	19.2	29.8	0.515	C	S.-i. Fujiwara, personal observation
	<i>T. tetradactyla</i>	UMZC E.581	49.1	16.5	25.1	0.515	C	S.-i. Fujiwara, personal observation
	<i>T. sp.</i>	IC	47.9	13.7	24.0	0.501	C	S.-i. Fujiwara, personal observation
Dermoptera								
Cynocephalidae	<i>Cynocephalus variegatus</i>	ZRC 4.8187*	42.4	21.4	6.8	0.161	F	Grassé (1955) and Lim (2007)
	<i>C. variegatus</i>	ZRC 4.9464*	19.4	10.6	3.7	0.191	F	Grassé (1955) and Lim (2007)
	<i>C. variegatus</i>	ZRC 4.8119*	44.9	21.5	6.9	0.154	F	Grassé (1955) and Lim (2007)
	<i>C. variegatus</i>	ZRC 4.8112*	31.4	15.4	6.1	0.194	F	Grassé (1955) and Lim (2007)
Primates								
Lemuridae	<i>Varecia sp.</i>	NSM M 33114	39.7	19.6	15.9	0.401	B	Nowak (1999)
Loridae	<i>Nycticebus coucang</i>	NSM M 35960*	11.2	5.4	3.8	0.336	C	Jouffroy & Petter (1990)
	<i>N. coucang</i>	NSM M 36100*	31.7	10.8	6.6	0.207	C	Jouffroy & Petter (1990)

Table 2 (Continued).

Taxonomy			Moment arms (mm)			MAR		
Order/family	Taxa	Specimen	Fl ₁	Fl ₂	Ex	Ex/Fl	LA	References
Cercopithecidae	<i>N. coucang</i>	KPM 3674*	27.6	12.8	6.7	0.243	C	Jouffroy & Petter (1990)
	<i>Macaca fuscata</i>	KPM 4191*	50.6	33.3	24.1	0.477	B	Nowak (1999)
Pongidae	<i>Pongo pygmaeus</i>	NSM M 31996	120.6	61.8	27.4	0.227	C	Thorpe & Crompton (2006)
	<i>P. pygmaeus</i>	NSM M 4226	110.9	58.2	24.4	0.220	C	Thorpe & Crompton (2006)
Hominidae	<i>Pan troglodytes</i>	NSM M 33042	91.8	61.8	33.0	0.360	B	Nowak (1999)
	<i>P. troglodytes</i>	NSM M 32559	88.8	58.6	31.8	0.358	B	Nowak (1999)
Lagomorpha								
Leporidae	<i>Oryctolagus cuniculus</i>	NSM M 35751	9.9	10.8	10.7	0.991	A	Nowak (1999)
	<i>Lepus brachyurus</i>	NSM unnumbered	9.9	9.3	12.6	1.279	A	Nowak (1999)
Rodentia								
Sciuridae	<i>Petaurista leucogenys</i>	NSM PO 94	23.5	13.9	8.2	0.348	C	S.-I. Fujiwara, personal observation
	<i>P. leucogenys</i>	KPM unnumbered*	16.5	12.3	5.8	0.350	C	S.-I. Fujiwara, personal observation
Gliridae	<i>Glirulus japonicus</i>	NSM unnumbered*	3.7	3.8	2.6	0.680	C	Minato 2009 pers. comm.
	<i>Graphiurus murinus</i>	UMUT unnumbered*	3.8	3.4	2.5	0.647	C	S.-I. Fujiwara, personal observation
Caviidae	<i>Cavia porcellus</i>	NSM M 35862	8.3	7.4	8.8	1.060	A	Weisbecker & Schmid (2007)
	<i>Dolichotis patagonum</i>	NSM M 35831	23.1	22.1	26.7	1.154	A	Weisbecker & Schmid (2007)
Hystricidae	<i>Erethizon dorsatum</i>	NSM M 34319	26.6	21.1	13.7	0.514	B	Weisbecker & Schmid (2007)
Soricomorpha								
Talpidae	<i>Mogera kobeeae</i>	NSM PO 123	5.3	3.6	9.5	1.792	D	Nowak (1999)
Cetartiodactyla								
Suidae	<i>Sus scrofa</i>	KPM 3681*	36.5	22.6	53.9	1.477	A	Nowak (1999)
	<i>S. scrofa domesticus</i>	UMUT unnumbered*	39.0	40.2	53.8	1.339	A	Nowak (1999)
Tayassuidae	<i>Tayassu tajacu</i>	UMUT 0279	28.4	21.1	46.8	1.646	A	Nowak (1999)
Giraffidae	<i>Giraffa camelopardalis</i>	KPM 3928*	81.0	71.6	64.8	0.800	A	Nowak (1999)
	<i>G. camelopardalis</i>	UMUT unnumbered	65.5	119.0	147.3	1.238	A	Nowak (1999)
Cervidae	<i>Rangifer tarandus</i>	UMUT 0036	51.7	46.3	65.8	1.273	A	Nowak (1999)
Bovidae	<i>Bos gaurus</i>	KPM 3937*	113.0	65.8	132.2	1.170	A	Nowak (1999)
	<i>Bubalus bubalis</i>	UMUT unnumbered	89.7	108.1	131.9	1.215	A	Nowak (1999)
Carnivora								
Mustelidae	<i>Gulo gulo</i>	NSM M 35843	42.8	30.4	27.3	0.637	B	Van Vankenburgh (1987)
	<i>Lutra lutra</i>	NSM M 33858	20.2	14.4	16.5	0.817	B	Leblanc (2003)
	<i>Enhydra lutris</i>	UMUT unnumbered*	39.1	25.9	21.0	0.538	A	Iwaniuk (2000)
Ailuridae	<i>Ailurus fulgens</i>	NSM M 34320	29.9	19.8	16.9	0.565	B	Iwaniuk (2000)
Ursidae	<i>Ailuropoda melanoleuca</i>	NSM M 32901	111.1	54.2	56.2	0.506	B	Iwaniuk (2000)
	<i>Tremarctos ornatus</i>	NSM M 22995	87.5	48.8	56.3	0.643	B	Van Vankenburgh (1987)
	<i>Melursus ursinus</i>	NSM M 25234	101.1	49.5	60.1	0.595	B	Van Vankenburgh (1987)
	<i>Ursus maritimus</i>	NSM M 31634	112.0	61.8	70.1	0.626	A	Iwaniuk (2000)
	<i>U. maritimus</i>	UMUT unnumbered*	149.0	102.0	99.1	0.665	A	Iwaniuk (2000)
Canidae	<i>Nyctereutes procyonoides</i>	NSM M 35491	20.0	18.9	19.0	0.944	B	Kauhala & Saeki (2004)
	<i>Chrysocyon brachyurus</i>	NSM M 16003	48.0	40.4	41.1	0.856	A	Iwaniuk (2000)
	<i>C. brachyurus</i>	NSM M 36655*	55.4	38.5	43.3	0.781	A	Iwaniuk (2000)
	<i>Canis familiaris</i>	UMUT unnumbered*	56.1	41.0	53.3	0.950	A	Van Vankenburgh (1987)
Herpestidae	<i>Mungos mungo</i>	NSM M 35866	21.8	11.4	12.3	0.566	A	Gittleman (1986)
Felidae	<i>Helogale parvula</i>	NSM M 35753	12.2	6.1	6.7	0.549	B	Iwaniuk (2000)
	<i>Felis catus</i>	NSM M 35590	23.5	17.9	17.5	0.744	B	Nowak (1999)
	<i>Pronailurus bengaliensis</i>	NSM M 14329	12.0	12.9	12.2	0.946	B	Iwaniuk (2000)
	<i>Leptailurus serval</i>	NSM M 27664	46.7	25.7	26.8	0.574	B	Nowak (1999)
	<i>Caracara caracal</i>	NSM M 2609	30.8	21.0	26.3	0.855	B	Van Vankenburgh (1987)
	<i>Acinonyx jubatus</i>	NSM M 31465	60.7	29.7	47.4	0.780	B	Van Vankenburgh (1987)
	<i>A. jubatus</i>	NSM M 31466	49.2	29.6	45.2	0.918	B	Van Vankenburgh (1987)
	<i>A. jubatus</i>	NSM M 36698 *	56.9	67.8	47.1	0.694	B	Van Vankenburgh (1987)
	<i>Neofelis nebulosa</i>	NSM M 31826	43.7	30.5	30.9	0.706	B	Van Vankenburgh (1987)
	<i>Uncia uncia</i>	NSM M 33876	54.2	33.9	44.2	0.816	B	Iwaniuk (2000)
<i>Panthera pardalis</i>	KPM 3653*	99.3	48.4	54.2	0.528	B	Van Vankenburgh (1987)	

Table 2 (Continued).

Taxonomy			Moment arms (mm)			MAR		
Order/family	Taxa	Specimen	Fl ₁	Fl ₂	Ex	Ex/Fl	LA	References
	<i>P. tigris</i>	NSM M 33189	87.6	62.7	75.3	0.859	B	Van Vankenburg (1987)
	<i>P. leo</i>	NSM M 33055	83.7	59.9	66.7	0.797	B	Van Vankenburg (1987)
Perissodactyla								
Equidae	<i>Equus caballus</i>	NSM PO 131	72.0	105.0	109.5	1.043	A	Nowak (1999)
	<i>E. caballus</i>	NSM M 36001*	65.6	67.6	103.0	1.524	A	Nowak (1999)
	<i>E. asinus</i>	KPM 3932*	69.4	83.9	86.4	1.030	A	Nowak (1999)
Tapiridae	<i>Tapirus indicus</i>	KPM 3936*	64.3	61.6	88.5	1.376	A	Nowak (1999)
Chiroptera								
Pteropodidae	<i>Pteropus pselaphon</i>	NSM M 35961*	15.3	10.2	5.8	0.376	F	S.-I. Fujiwara, personal observation
	<i>P. sp.</i>	UMUT unnumbered*	16.6	4.1	7.7	0.462	F	S.-I. Fujiwara, personal observation
	<i>Rousettus aegyptiacus</i>	NSM M 34803	9.8	8.0	3.4	0.347	F	S.-I. Fujiwara, personal observation

Institution abbreviations: IC, personal collection of N. Inuzuka, Graduate School of Medicine, The University of Tokyo, Tokyo, Japan; KPM, Kanagawa Prefectural Museum, Odawara, Japan; NSM, National Science Museum, Tokyo, Japan; UMUT, The University Museum, the University of Tokyo, Japan; UMZC, University Museum of Zoology, Cambridge, UK; ZRC, Zoological Collection, Raffles Museum of Biodiversity Research, Singapore.

*Measurements taken from carcasses. MAR is calculated as (Ex/Fl₁) or (Ex/Fl₂), whichever is smaller.

length (Gans & Bock, 1965; Payne et al. 2005; Williams et al. 2007, 2008). Thus our qualitative conclusions about the differences of extensor: flexor muscle masses in suspended vs. upright taxa should be sufficiently reliable.

Results

Do suspended quadrupeds match their elbow joint angles to maximize flexor muscle moment arms?

Our motion analyses revealed that the elbow joints of *Choloepus*, *Pteropus* and *Nycticebus* are well flexed, below 120°, during the adducted portion of the stance phase (Fig. 7A,B,D). The elbow joint angle at mid-stance, where the ground reaction force is expected to be maximal (e.g. Biewener, 1989, 1990; Ishida et al. 1990), was flexed to a 60–100° angle at least during the periods when the humeri were more adducted at mid-stance (Fig. 7A,B,D). The elbow joint in the abducted portion was relatively extended, but the actual angles in the abducted portion are expected to be less than the measured angles (dotted lines in Fig. 7A,B,D).

The elbows of *Choloepus*, *Pteropus*, *Nycticebus* and *Cynocephalus* were flexed mostly below 80° (similar to mid-stance) in static postures when they were resting or sleeping, except for a few cases in *Nycticebus*, where the elbows were extended up to 130° when the animal was alert and actively inspecting its surroundings (Fig. 7).

The elbows in other suspended quadrupeds, such as *Bradypus* and *Pongo*, can be fully extended to about 180° (e.g. Nowak, 1999; Thorpe & Crompton, 2006) but according to our manipulations of carcasses the elbows of our

four study genera can only extend to 110–150° (Fig. 7). The ranges of elbow joint motions are restricted not only by the muscles and tendons, but also by the geometry of the joint surfaces.

The relative position of Lsc (the origin of Fl₂) on the humerus does not vary between our study taxa; its position remains on the distal third of the humeral shaft in lateral views (Fig. 8A–D). Therefore, the estimated elbow joint angles where the Fl₂ moment arms are maximized do not vary appreciably between our study taxa. On the other hand, the relative position of Rt (the insertion of Fl₁) varies more widely between the four genera. In the antebrachia of *Pteropus*, *Cynocephalus* (fixed antebrachium) and *Choloepus* (even in pronated or semi-supinated positions) the *M. biceps brachii* (Fl₁) insertion (Rt) spanned the space between the radius and the ulna (Fig. 8A–D). However, in *Nycticebus* the relative position of Rt is located cranially in accordance with supination of the antebrachia (Fig. 7D). Consequently, the estimated elbow joint angle where the Fl₁ moment arm is maximized showed interspecific variation: the optimal angles are at about 70° in *Choloepus*, *Pteropus* and *Cynocephalus*, and at about 90° in *Nycticebus* (Figs 7 and 8).

Considering the observed angles *in vivo* and the ranges of motion allowed at the elbow, the elbow joints of all four study taxa were neither maximally extended nor flexed, at least during the adducted portion of the stance phase. Most importantly, the estimated moment arm-maximizing angles for both Fl₁ and Fl₂ and the observed angles were close to each other, especially in *Choloepus*, *Pteropus* and *Cynocephalus* (Fig. 7A–C). In *Nycticebus*, the optimal elbow joint angle estimated for the Fl₂ moment arm was close to the

Type A: Upright non-scansorial quadrupeds

1a	1b	1c	1d	3	D	B	A	<i>Canis lupus familiaris</i> (UMUT unnumbered)		
1a		1b	1c		D	B	A	<i>Hippopotamus amphibius</i> (J. R. Hutchinson pers. coll.)		
1a		1c	3		D	B	A	<i>Elephas maximus</i> (J. R. Hutchinson pers. coll.)		
1a	1b	1c	1d	3	D	B	A	<i>Chrysocyon brachyurus</i> (NSM M 16003)		
2	1a	1b	1c	3	D	B	A	<i>Sus scrofa domesticus</i> (UMUT unnumbered)		
2	1a	1b	1c	3	D	B	A ₁ A ₂	<i>Ursus maritimus</i> (UMUT unnumbered)		
	1+3				D	B	A	<i>Sus scrofa</i> (KPM 3681)		
1a	1b	1c			D	B	A	<i>Oryctolagus cuniculus</i> (UMUT unnumbered)		
1a	1b	1c	3		D	C	B	A	<i>Loxodonta africana</i> (J. R. Hutchinson pers. coll.)	
1a	1b	1c			D	B	A	<i>Equus caballus</i> (NSM M 36001)		
2	1a	1b	1c	3	D	B	A	<i>Tapirus indicus</i> (KPM 3936)		
2	1a	1b	1c	3	D	B	A	<i>Equus asinus</i> (KPM 3932)		
	1+3				D	B	A	<i>Bos gaurus</i> (KPM 3937)		
1a	1b	1c	3		D	B	A	* <i>Giraffa camelopardalis</i> (KPM 3928)		
1a	1c	1b	1e	1d	3	D	C	B	A	<i>Macropus giganteus</i> (UMUT unnumbered)
1a	1b	1c	3		D	B	A	* <i>Rhinoceros unicornis</i> (J. R. Hutchinson pers. coll.)		
1a	1b	1c	3		D	B	A ₁ A ₂	<i>Giraffa camelopardalis</i> (JRHutchinson pers. coll.)		
2	1a	1b	1c	1d	3	D	C	B	A	<i>Enhydra lutris</i> (UMUT unnumbered)
1a	1b	1c	3		D	C	B	A	* <i>Elephas maximus</i> (J. R. Hutchinson pers. coll.)	

Type B: Upright scansorial but non-suspended quadrupeds

2	1a	1b	1c	3	D	B	A	<i>Acinonyx jubatus</i> (NSM M 36698)
1a	1b	1c	3	D	C	B	A	<i>Macaca fuscata</i> (KPM 4191)
1a	1b	1c	1d	3	D	B	A	<i>Panthera pardalis</i> (KPM 3653)

Type C: Upright suspended quadrupeds

1a	1b	1c			D	B	A	<i>Graphiurus murinus</i> (UMUT unnumbered)								
2	1a	1b	1c	3	D+C	B	A	<i>Nycticebus coucang</i> (KPM 3674)								
	1				D+C	B	A	<i>Nycticebus coucang</i> (NSM M 36100)								
2	1a	1b+c			D	C	B	A	<i>Petaurista leucogenys</i> (KPM unnumbered)							
1a	1b	1c			D	B	A	* <i>Glirulus japonicus</i> (NSM M unnumbered)								
2	1a	1b	5	4	3	H	D	K	J	I	C ₂	C ₁	B	A	A ₂	<i>Tamandua tetradactylus</i> (UMUT unnumbered)
	1					D+C	B	A	* <i>Nycticebus coucang</i> (NSM M 35960)							

Type F: Non-upright suspended quadrupeds

2	1a	1b	1c+3		D	C	B	A	* <i>Cynocephalus variegatus</i> (ZRC 4.9464)				
	1				D+C	B	A	<i>Pteropus pselaphon</i> (NSM M 35961)					
1a	1b	1c			D+C	B	A ₁	A ₂	<i>Pteropus</i> sp. (UMUT unnumbered)				
1a	1b	1c			D	C	B	A ₁	A ₂	<i>Pteropus</i> sp. (UMUT unnumbered)			
2	1a	1b	1c+3		D	C	B	A	<i>Cynocephalus variegatus</i> (ZRC 4.8183)				
1a	1b	1c	3	4	I+H	G	D	C	B	A	F	E	<i>Choloepus didactylus</i> (UMUT unnumbered)
1a	1b	1c	3	4	I	H	G	D	C	B	A	F	* <i>Choloepus didactylus</i> (UMUT unnumbered)
2	1a	1b	1c	3	D	C	B	A	<i>Cynocephalus variegatus</i> (ZRC 4.8187)				



Fig. 6 Muscle mass ratios of elbow joint extensors (Ex) and flexors along the brachium (Fl₁) and antebrachium (Fl₂). The length of each bar represents the relative mass of each muscle, when the total mass of the extensors and flexors of an individual is 100% (see bottom bar for abstract example). No data were obtainable for taxa in types D and E. Asterisks indicate juvenile specimens. (1) *M. triceps brachii* (1a, long head; 1b, lateral head; 1c, medial head; 1d, accessory head; 1e, intermediate head); (2) *M. dorsipectoralis*; (3) *M. anconeus*; (4) *M. epitrochleoanconeus*; (5) *M. flexor carpi ulnaris*. A, *M. biceps brachii* (A₁, short head; A₂, long head); B, *M. brachialis*; C, *M. brachioradialis* (C₁, short head; C₂, long head); D, *M. extensor carpi radialis*; E, *M. cleidobrachialis*; F, *M. ectoantebrachialis*; G, *M. supinator*; H, *M. pronator teres*; I, *M. flexor carpi radii*; J, *M. flexor digiti profundus*; K, *M. flexor digiti sublimis*. See institution abbreviations in Tables 1 and 2.

observed angles in static postures, whereas the optimal angle estimated for the Fl₁ moment arm was close (< 20 ° difference) to the angles observed at mid-stance of locomo-

tion (Fig. 7D). Overall, our first hypothesis is well supported, although elbow joint function in *Nycticebus* deserves more investigation.

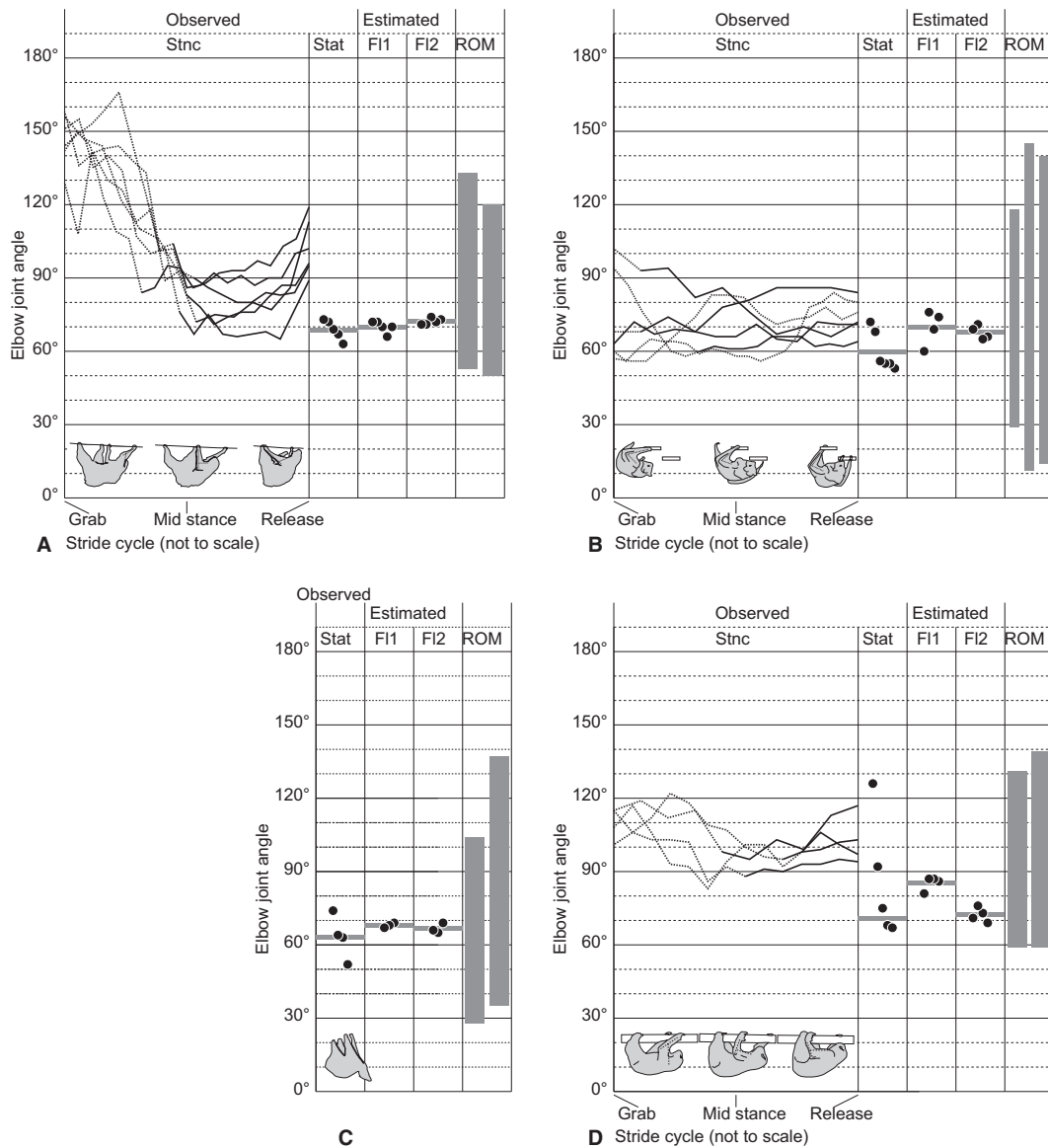


Fig. 7 (A–D) Observed elbow joint angles, including the changes of the joint angle during stance phase (Stnc) and the angle in static postures (Stat), estimated elbow joint angles where the moment arms of the flexors along the brachium (F₁) and the antebrachium (F₂) are maximized, and the ranges of elbow joint motion (ROM), are compared for our study taxa of four suspended quadrupeds: (A) *Choloepus*, (B) *Pteropus*, (C) *Cynocephalus* (no Stnc data recorded) and (D) *Nycticebus*. Solid and dotted lines of the transitions in Stnc indicate, respectively, the portions of the stance phase where the humerus is more abducted (first half) or adducted (second half). The horizontal bar in each section of Stat, F₁ and F₂ is a mean value of the measurements.

Do suspended quadrupeds have larger flexor vs. extensor muscle masses and moment arms?

The elbow extensor/flexor muscle moment arm ratios of quadrupeds varied between the different categories of locomotor abilities, descending (i.e. more strongly emphasizing flexors) in order from type A, to B, to C, to F (using median values; Figs 9 and 10A). There were only three data points for taxa in type D, so clear conclusions about this group cannot be drawn, although they were most similar to type A (Fig. 10A). No animals categorized in type E could

be obtained for measurement. The ranges of the elbow joint extensor/flexor moment arm ratio do not overlap between types A (upright non-scansorial taxa) and F (non-upright suspended quadrupeds). The median extensor/flexor muscle moment arm ratios were four times smaller for our study taxa (type F) vs. type A.

Similarly, the median value of extensor/flexor muscle mass ratio decreased (i.e. more strongly emphasized flexors) in order from type A, to C, to F (Fig. 10B). There were only three samples for type B taxa but the muscle mass ratio was larger than in types C and F (Fig. 10B). Unfortunately, no

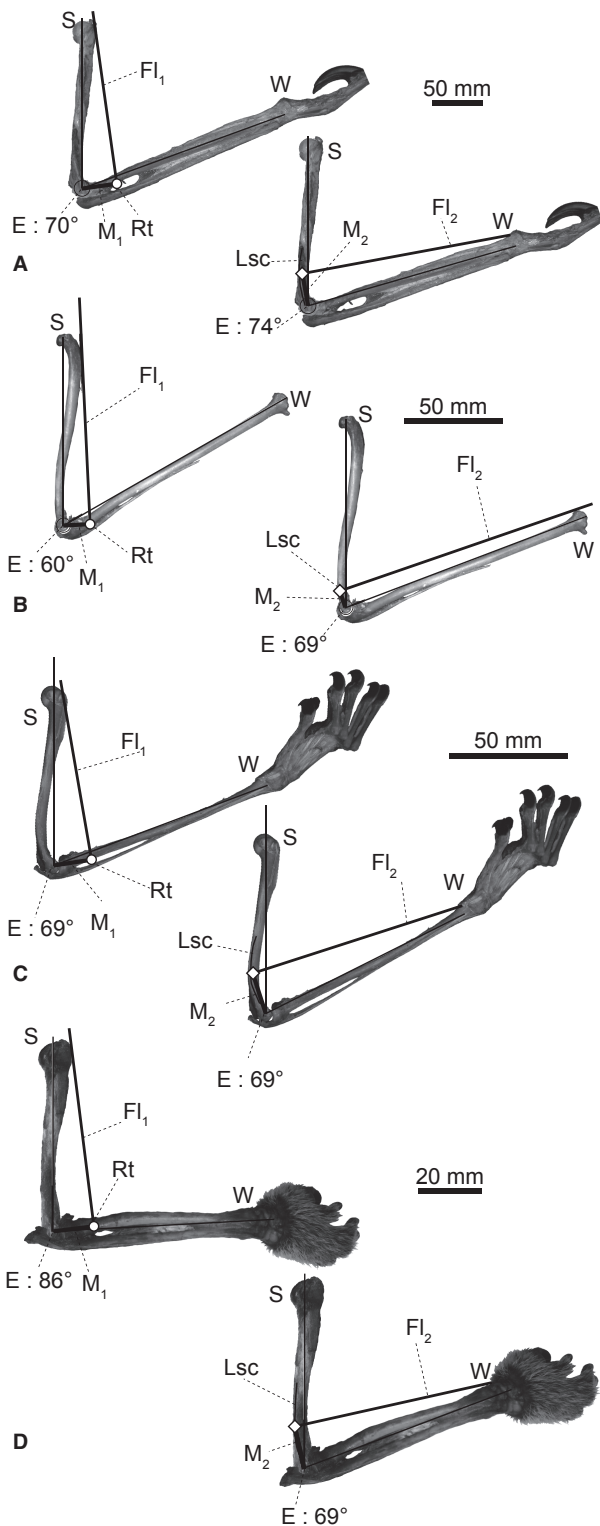


Fig. 8 Estimated elbow joint angles (maximizing flexor moment arms) for the FI_1 and FI_2 muscles of selected specimens. ROM was measured after the flight membrane was removed in *Pteropus* specimens: (A) *Choloepus hoffmanni* (UMUT unnumbered), (B) *Pteropus dasymallus* (NSM PO 127), (C) *Cynocephalus variegatus* (ZRC 4.8112) and (D) *Nycticebus coucang* (KPM 3674). The antebrachia of *Choloepus* and *Nycticebus* specimens are held in semi-supinated position. E, centre of elbow joint rotation; Lsc, lateral supracondylar crest; Rt, radial tuberosity; S and W, shoulder and wrist joints, respectively.

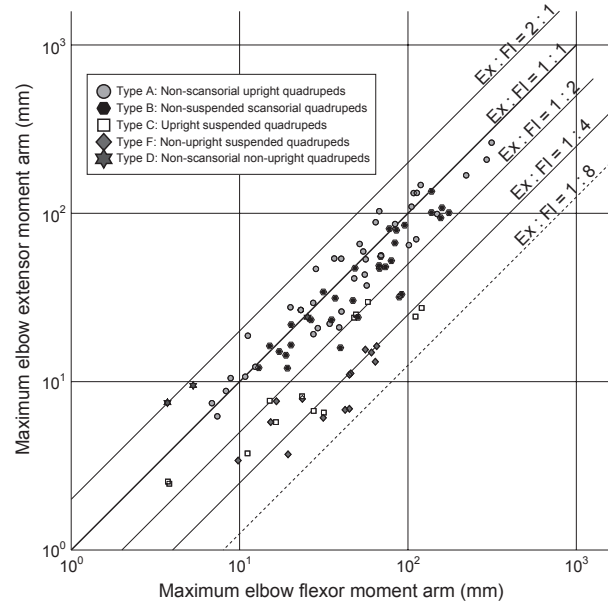


Fig. 9 Comparison between maximum possible moment arms of the elbow joint extensor (Ex: vertical axis) and flexor (FI_1 or FI_2 , whichever is larger: horizontal axis) muscles. See Figs 3 and 5 and main text for the details of the measurements and the locomotor ability categories. Animals plotted on the upper left possess relatively large extensor moment arms (e.g. upright quadrupeds), and the one on lower right possesses relatively large flexor moment arms (e.g. suspended quadrupeds).

samples were available for types D or E. However, for type A taxa, the flexor masses were relatively large in some species with additional locomotor abilities, such as in *Macropus* (habitual bipeds), *Enhydra* (amphibious) and *Giraffa* ('normal' upright quadruped, but with relatively long distal

elements that may require large flexor torques for limb protraction), and in a juvenile (but not adult) *Elephas* and *Ceratotherium*. Overall, our second hypothesis remains well supported by our results: much like the moment arm ratios, the median values for extensor/flexor muscle mass ratios in suspended, non-upright quadrupeds were approximately four times smaller than those for upright non-scansorial taxa (type A). We did not find conclusively significant correlations between body mass and the elbow extensor/flexor muscle moment arm or muscle mass ratio within each type (see Supporting Information Data S1, Tables S1–S4, Figs S2 and S3).

Discussion and Conclusions

We find that suspended quadrupeds use poses that are approximately optimal for supporting their elbow joints

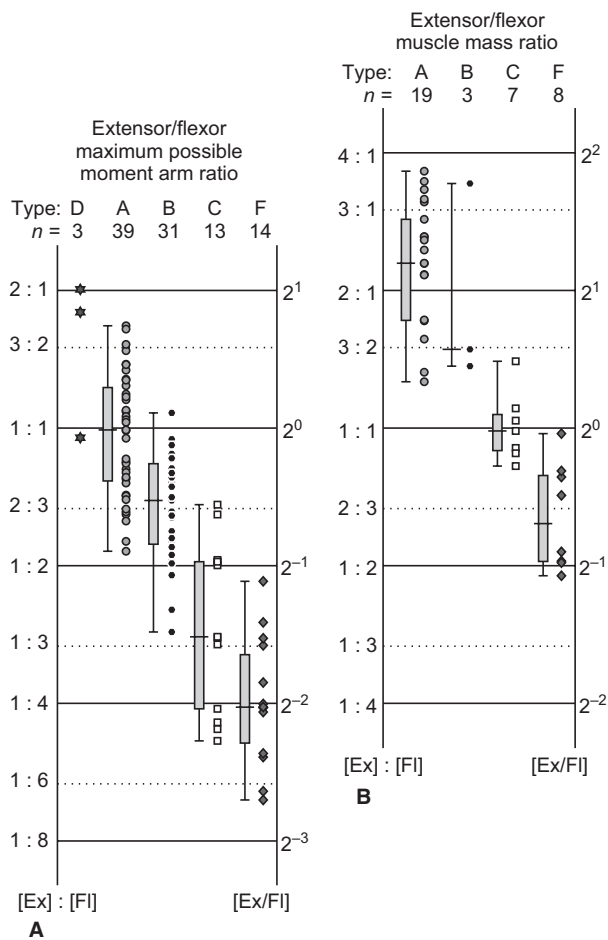


Fig. 10 Elbow joint extensor/flexor ratios for (A) maximum possible moment arm and (B) total muscle masses. Extensor (Ex) and flexor (Fl) ratios are plotted along the vertical axis, and quartiles for each type of locomotor ability are shown in box plots.

during locomotion (i.e. maximizing flexor muscle moment arms) and that their morphology has evolved to match these demands, increasing the relative leverages and masses of flexor vs. extensor muscles. Therefore, in both upright (Fujiwara, 2009) and suspended (this study) postures, the moment arms of antigravity muscles are a key factor in the selection of elbow joint poses in extant quadrupeds as in some other taxa (Lieber, 1997; Hutchinson et al. 2005; Johnson et al. 2008).

We might expect then that the application of biomechanical theory proposed for normal, non-inverted taxa (see Introduction) would still hold for the response of the musculoskeletal system to gravitational constraints in suspended quadrupeds, but with one major change. Flexor, rather than extensor, muscles dominate the antigravity support role in these taxa, and thus changes predicted for flexor (i.e. leg-swinging) muscles in normal taxa should apply to extensor muscles in suspended quadrupeds (e.g. Cohen & Gans, 1975; Tuttle et al. 1983; Jouffroy & Stern, 1990; Payne et al. 2005; Williams et al. 2007). This condition

has evolved convergently in at least our four study taxa, and we predict that this will hold for all other extant suspended quadrupeds.

As far as upright, scansorial and suspended quadrupedal abilities are concerned, our analyses support the notion that there are mechanical trade-offs between locomotor abilities. Our locomotor types A and F are drastically different in these abilities and their specializations in extensor vs. flexor muscles of the elbow may be integral to these differences. However, as we acknowledged in the Introduction, biomechanical factors other than the muscle moment arm (e.g. muscle properties and gravitational or ground reaction force moment arms) are important determinants of the elbow and other joint angles that animals use. We find it exciting and a bit surprising that even suspended quadrupeds tend to adopt postures in which their elbow flexor muscle moment arms are near maximal and hence that component of their antigravity support is optimized. Yet the interplay of this component and others remains to be fully determined for any species or behaviour.

Regardless, our study shows how the inverted lifestyle of suspended quadrupeds has inverted the 'normal' biomechanical functions of their antigravity vs. leg-swinging muscles. Their muscular changes have made them adroit at this upside-down lifestyle, but at the repeatedly evolved cost of reducing or even losing the ability to support themselves in the upright posture of their distant common mammalian ancestors.

Acknowledgements

This paper was supported by the Japan Society of Promotion for Science (Grant number: 22-4730). We also thank S. Kawada (NSM), H. Taru (KPM), K. K. P. Lim (ZRC), N. Lim (University of California, Davis), and M. Lowe (UMZC) for providing the specimens for dissection and measurements, M. Ohga (Ueno Zoo) for giving us the opportunity to film at Ueno Zoo, A. Hayashida (Kobe Oji Zoo), D. Koyabu, Y. Nakajima, K. Mori, N. Miwa and M. Hosojima (The University of Tokyo) for assisting with the dissections, R. Matsumoto (University College London), N. Egi (Kyoto University) and G. Suwa (The University of Tokyo) for providing critical literature, T. Kubo (Fukui Prefectural Dinosaur Museum) for assisting with filming at zoos, A. Spence (Royal Veterinary College), G. Byrnes (University of California, Berkeley), N. Inuzuka (The University of Tokyo), M. Takai (Primate Research Institute, Kyoto University) and S. Minato (Yamane Museum) for their helpful advice, and three anonymous reviewers for improving this paper. J.R.H. thanks the BBSRC for funding via grants BB/C516844/1, BB/F001169/1 and BB/H002782/1.

References

- Airapetyants AE, Fokin IM (2003) Biology of European flying squirrel *Pteromys volans* L. (Rodentia: Pteromyidae) in the North-West of Russia. *Russ J Theriol* 2, 105–113.
- Alexander RM (1984) The gaits of bipedal and quadrupedal animals. *Int J Rob Res* 3, 49–59.

- An KN, Takahashi K, Harrigan TP, et al. (1984) Determination of muscle orientations and moment arms. *J Biomech Eng ASME* **106**, 280–282.
- Autumn K, Sitti M, Liang YA, et al. (2002) Evidence for van der Waals adhesion in gecko setae. *PNAS* **99**, 12252–12256.
- Biewener AA (1989) Scaling body support in mammals: limb posture and muscle mechanics. *Science* **245**, 45–48.
- Biewener AA (1990) Biomechanics of mammalian locomotion. *Science* **250**, 1097–1103.
- Biewener AA (2005) Biomechanical consequences of scaling. *J Exp Biol* **208**, 1665–1676.
- Cant JGH (1987) Positional behaviour of female Bornean orangutans (*Pongo pygmaeus*). *Am J Primatol* **12**, 71–90.
- Channon AJ, Crompton RH, Gunther MM, et al. (2010) Muscle moment arms of the gibbon hind limb: implications for hylobatid locomotion. *J Anat* **216**, 446–462.
- Cohen AH, Gans C (1975) Muscle activity in rat locomotion: movement analysis and electromyography of the flexors and extensors of the elbow. *J Morphol* **146**, 177–196.
- Dickinson MH, Farley CT, Full RJ, et al. (2002) How animals move: an integrative view. *Science* **288**, 100–106.
- Fujiwara S-I (2009) Olecranon orientation as an indicator of elbow joint angle in the stance phase, and estimation of forelimb posture in extinct quadruped animals. *J Morphol* **270**, 1107–1121.
- Gans C, Bock WJ (1965) The functional significance of muscle architecture — a theoretical analysis. *Ergeb Anat Entwicklungsgesch* **38**, 115–142.
- Gittleman JL (1986) Carnivore brain size, behavioral ecology, and phylogeny. *J Mamm* **67**, 23–36.
- Godfrey LR, Jungers WL (2003) The extinct sloth lemurs of Madagascar. *Evol Anthropol* **12**, 252–263.
- Graham KM, Scott SH (2003) Morphometry of *Macaca mulatta* forelimb. III. Moment arm of shoulder and elbow muscles. *J Morphol* **255**, 301–314.
- Grassé PP (1955) Ordre des dermoptères. In: *Traité de Zoologie, Anatomie, Systématique, Biologie, Tome XVII Mammifères: Systématique et Ethologie*. (ed. Grassé PP), pp. 1713–1728. Paris: Libraires de l'Académie de Médecine.
- Gregersen CS, Silverton NA, Carrier DR (1998) External work and potential for elastic storage at the limb joints of running dog. *J Exp Biol* **201**, 3197–3210.
- Hutchinson JR, Anderson FC, Blemker S, et al. (2005) Analysis of hindlimb muscle moment arms in *Tyrannosaurus rex* using a three-dimensional musculoskeletal computer model. *Paleobiol* **31**, 676–701.
- Ishida H, Jouffroy FK, Nakano Y (1990) Comparative dynamics of pronograde and upside down horizontal quadrupedalism in the slow loris (*Nycticebus coucang*). In: *Gravity, Posture and Locomotion in Primates*. (eds Jouffroy FK, Stack MH, Niemitz C), pp. 209–220. Florence: Il Sedicesimo.
- Iwaniuk AN (2000) *The Evolution of Skilled Forelimb Movements in Carnivores*. Msc Thesis, Canada: University of Lethbridge.
- Jenkins FA, Weijs WA (1979) The functional anatomy of the shoulder in the Virginia opossum (*Didelphis virginiana*). *J Zool Lond* **188**, 379–410.
- Johnson WL, Jindrich DL, Roy RR, et al. (2008) A three-dimensional model of the rat hindlimb: musculoskeletal geometry and muscle moment arms. *J Biomech* **41**, 610–619.
- Jouffroy FK, Petter A (1990) Gravity-related kinematic changes in lorine horizontal locomotion in relation to position of body. In: *Gravity, Posture and Locomotion in Primates*. (eds Jouffroy FK, Stack MH, Niemitz C), pp. 199–208. Florence: Il Sedicesimo.
- Jouffroy FK, Stern JT (1990) Telemetered EMG study of the antigravity versus propulsive actions of knee and elbow muscles in the slow loris (*Nycticebus coucang*). In: *Gravity, Posture and Locomotion in Primates*. (eds Jouffroy FK, Stack MH, Niemitz C), pp. 221–236. Florence: Il Sedicesimo.
- Jungers WL, Stern JT (1980) Telemetered electromyography of forelimb muscle chains in gibbons (*Hylobates lar*). *Science* **208**, 617–619.
- Jungers WL, Stern JT (1981) Preliminary electromyographical analysis of brachiation in gibbon and spider monkey. *Int J Primatology* **2**, 19–33.
- Kauhala K, Saeki M (2004) Finnish and Japanese raccoon dogs — on the road to speciation? In: *Biology and Conservation of Wild Canids*. (eds Macdonald DW, Sillero-Zubiri C), pp. 215–226. Oxford: Oxford University Press.
- Kikuchi Y (2010) Quantitative analysis of variation in muscle internal parameters in crab-eating macaques (*Macaca fascicularis*). *Anthropol Sci* **118**, 9–21.
- Kram R, Taylor CR (1990) Energetics of running: a new perspective. *Nature* **346**, 265–267.
- Lammers AR, Gauntner T (2008) Mechanics of torque generation during quadrupedal arboreal locomotion. *J Biomech* **41**, 2388–2395.
- Leblanc F (2003) Protecting fish farms from predation by the Eurasian otter (*Lutra lutra*) in the Limousin region of central France: first results. *IUCN Otter Spec Group Bull* **20**, 31–34.
- Lieber RL (1997) Muscle fiber length and moment arm coordination during dorsi- and plantarflexion in the mouse hindlimb. *Acta Anat* **159**, 84–89.
- Lim N (2007) *Colugo: The Flying Lemur of South-East Asia*. Singapore: Draco Publishing, National University of Singapore.
- Losos JB, Walton BM, Bennett AF (1993) Trade-offs between sprinting and clinging ability in Kenyan chameleons. *Funct Ecol* **7**, 281–286.
- Lucae JCG (1884) Statik und Mechanik der Quadrupeden an dem Muskeln des Lemur und *Choloepus*. *Abhandl Senckenberg Naturforsch Gesellsch Frankfurt* **13**, 1–92.
- McClarn D (1992) Locomotion, posture, and feeding behavior of kinkajous, coatis, and raccoons. *J Mamm* **73**, 245–261.
- Mendel FC (1981) Use of hands and feet of two-toed sloths (*Choloepus hoffmanni*) during climbing and terrestrial locomotion. *J Mamm* **62**, 413–421.
- Mendel FC (1985) Use of hands and feet of three-toed sloths (*Bradypus variegatus*) during climbing and terrestrial locomotion. *J Mamm* **66**, 359–366.
- Michilsens F, Vereecke EE, D'Août K, et al. (2010) Muscle moment arms and function of the siamang forelimb during brachiation. *J Anat* **217**, 521–535.
- Murray WM, Delp SL, Buchanan TS (1995) Variation of muscle moment arms with elbow and forearm position. *J Biomech* **28**, 513–525.
- Napier JR (1967) Evolutionary aspects of primate locomotion. *Am J Phys Anthropol* **27**, 333–341.
- Nowak RM (1999) *Walker's Mammals of the World*, 6th edn. Baltimore: The Johns Hopkins University Press.
- Nyakatura JA, Petrovitch A, Fischer MS (2010) Limb kinematics during locomotion in the two-toed sloth (*Choloepus didactylus*, Xenarthra) and its implications for the evolution of the sloth locomotor apparatus. *Zoology* **113**, 221–234.

- Payne RC, Hutchinson JR, Robilliard JJ, et al. (2005) Functional specialization of pelvic limb anatomy in horses (*Equus caballus*). *J Anat* **206**, 557–574.
- Reilly SM, McElroy EJ, Biknevicius AR (2007) Posture, gait and the relevance of locomotor costs and energy-saving mechanisms in tetrapods. *Zoology* **110**, 271–289.
- Russell EM (1986) Observations on the behaviour of the honey possum, *Tarsipes rostratus* (Marsupialia: Tarsipedidae) in captivity. *Aust J Zool Suppl Ser* **34**, 1–63.
- Salton JA, Sargis EJ (2009) Evolutionary morphology of the Tenrecoidea (Mammalia) hindlimb skeleton. *J Morphol* **270**, 367–387.
- Sargis EJ (2001) The grasping behaviour, locomotion and substrate use of the tree shrews *Tupaia minor* and *T. tana* (Mammalia, Scandentia). *J Zool Lond* **253**, 485–490.
- Spoor CW, Van Leeuwen JL (1992) Knee muscle moment arms from MRI and from tendon travel. *J Biomech* **25**, 201–206.
- Swartz SM, Bertram JEA, Biewener AA (1989) Telemetered *in vivo* strain analysis of locomotor mechanics of brachiating gibbons. *Nature* **342**, 270–272.
- Taylor BK (1978) The anatomy of the forelimb in the anteater (*Tamandua*) and its functional implications. *J Morphol* **157**, 347–368.
- Thorpe SKS, Crompton RH (2006) Orangutan positional behavior and the nature of arboreal locomotion in hominoidea. *Am J Phys Anthropol* **131**, 384–401.
- Thorpe SKS, Crompton RH, Gunther MM, et al. (1999) Dimensions and moment arms of the hind- and forelimb muscles of common chimpanzees (*Pan troglodytes*). *Am J Phys Anthropol* **110**, 179–199.
- Trapp GR (1972) Some anatomical and behavioural adaptations of ringtails, *Bassariscus astutus*. *J Mamm* **53**, 549–557.
- Tuttle R, Velte MJ, Basmajian JV (1983) Electromyography of brachial muscles in *Pan troglodytes* and *Pongo pygmaeus*. *Am J Phys Anthropol* **61**, 75–83.
- Van Vankenburgh B (1987) Skeletal indicators of locomotor behavior in living and extinct carnivores. *J Vert Paleont* **7**, 162–182.
- Weisbecker V, Schmid S (2007) Autopodial skeletal diversity in hystricognath rodents: functional and phylogenetic aspects. *Mamm Biol* **72**, 27–44.
- Weisbecker V, Warton DI (2006) Evidence at hand: diversity, functional implications, and locomotor prediction in intrinsic hand proportions of diprotodontian marsupials. *J Morphol* **267**, 1469–1485.
- Wickler SJ, Hoyt DF, Biewener AA, et al. (2005) *In vivo* muscle function vs speed. II. Muscle function trotting up an incline. *J Exp Biol* **208**, 1191–1200.
- Williams SB, Wilson AM, Payne RC (2007) Functional specialization of the thoracic limb of the hare (*Lepus europeus*). *J Anat* **210**, 491–505.
- Williams SB, Wilson AM, Daynes J, et al. (2008) Functional anatomy and muscle moment arms of the thoracic limb of an elite sprinting athlete: the racing greyhound (*Canis familiaris*). *J Anat* **213**, 373–382.
- Youlatos D (2002) Positional behaviour of black spider monkeys (*Ateles paniscus*) in French Guiana. *Int J Primatol* **23**, 1071–1093.
- Young RJ, Coelho CM, Wieloch DR (2003) A note on the climbing abilities of giant anteaters, *Myrmecophaga tridactyla* (Xenarthra, Myrmecophagidae). *Bol Mus Biol Mello Leitão* **15**, 41–46.

Supporting Information

Additional Supporting Information may be found in the online version of this article:

Data S1. The scaling of body mass and elbow extensor/flexor ratios of maximum muscle moment arms and masses in each locomotor type (A–F).

Fig. S1. Images from video clips of stance phases (from top to bottom) of (A) *Choloepus* and (B) *Pteropus* in near-frontal views, and (C) *Nycticebus* in lateral view. Bars on the right side of each image sequence indicate the phases of humeral abduction/adduction during the stance/swing phases of right (R) and left (L) forelimbs. The image sequences are not in equal intervals. See Fig. 4E for a representative image of *Cynocephalus*.

Fig. S2. Reduced major axis scaling plots for body mass and elbow extensor/flexor muscle moment arm ratios in locomotor types A–D and F. See Table S1 for the original data and Table S3 for the regression statistics.

Fig. S3. Reduced major axis scaling plots for body mass and elbow extensor/flexor muscle mass ratios in locomotor types A–C and F. See Table S2 for the original data and Table S4 for the regression statistics.

Table S1. Mean values of log extensor/flexor ratio of elbow joint muscle moment arms (Log Ex/FI), sample size (*n*), body mass (BM), mean value of the range of log body masses (Log BM), and locomotor ability (LA) in each study taxon. See main text and Fig. 5).

Table S2. Mean values of the log extensor/flexor ratio of elbow joint muscle masses (Log Ex/FI), sample size (*n*), body mass (BM), mean value of the range of log body masses (Log BM), and locomotor ability (LA) in each study taxon. See main text and Fig. 5).

Table S3. Sample size (*n*), correlation coefficient (*r*), coefficient of determination (*r*²) and significance probability (*P*) calculated by reduced major axis regression analysis of the relationship between body mass and elbow extensor/flexor muscle moment arm ratio in each locomotor type (A–D, and F: Fig. S2). See main text and Fig. 5.

Table S4. Sample size (*n*), correlation coefficient (*r*), coefficient of determination (*r*²), and significance probability (*P*) calculated by reduced major axis regression analysis of the relationship between body mass and elbow extensor/flexor muscle mass ratio in each locomotor type (A–C, and F: Fig. S3). See main text and Fig. 5.

As a service to our authors and readers, this journal provides supporting information supplied by the authors. Such materials are peer-reviewed and may be re-organized for online delivery, but are not copy-edited or typeset. Technical support issues arising from supporting information (other than missing files) should be addressed to the authors.